DTIC FILE COPY

UNLIMITED DISTRIBUTION

National Defence
Research and Development Branch

Défense nationale
Bureau de recherche et développement

TECHNICAL MEMORANDUM 91/203
January 1991

AD-A233 021

A DESIGN PROPOSAL FOR AN INEXPENSIVE PARAMETRIC ARRAY

F. D. Cotaras

DTIC
ELECTE
MAR 14 1991
D
E

Defence Research Establishment Atlantic

Centre de Recherches pour la Défense Atlantique

Canada

91 3 13 054

DEFENCE RESEARCH ESTABLISHMENT ATLANTIC

9 GROVE STREET
P.O. BOX 1012
DARTMOUTH, N.S.
B2Y 3Z7

TELEPHONE
(902) 426-3100

CENTRE DE RECHERCHES POUR LA DÉFENSE ATLANTIQUE

9 GROVE STREET
C.P. 1012
DARTMOUTH, N.É.
B2Y 3Z7

UNLIMITED DISTRIBUTION

National Defence
Research and Development Branch

Défense nationale
Bureau de recherche et développement

A DESIGN PROPOSAL FOR AN INEXPENSIVE PARAMETRIC ARRAY

F. D. Cotaras

January 1991

Approved by P. Bhartia
Director / Sonar Division

Distribution Approved by A.T. Ashley

A / Director / Sonar Division

TECHNICAL MEMORANDUM 91/203

Defence Research Establishment Atlantic

Centre de Recherches pour la Défense Atlantique

Canada

Abstract

In this Technical Memorandum, the fundamentals of the physics that govern the operation of parametric arrays are discussed in a non-mathematical way. The governing relations for a piston source as derived using linear theory are also discussed. These relations are contrasted with those that govern the source level and beamwidth of the parametric array which is linear absorption limited in the collimated zone near the source. A simple design for a low cost parametric array is presented, and its advantages and disadvantages are discussed.

Résumé

Dans ce mémoire technique, les fondements de la physique qui régit le fonctionnement des antennes-réseaux paramétriques sont discutés d'une manière non mathématique. Les relations régissant un piston source découlant de la théorie linéaire sont aussi discutées. Ces relations sont comparées à celles qui régissent le niveau de la source et la largeur du faisceau de l'antenne paramétrique qui est limitée a l'absorption linéaire dans la zone collimatée près de la source. Un modèle simple d'antenne paramétrique bon marché est présenté, et ses avantages et inconvénients sont discutés.

Contents

Accession For
NTIS GRA&I
DTIC TAB
Unannounced
Justification
By
Distribution/
Availability Codes
Dist | Avail and/or Special
A-1

QUALITY INSPECTED 3

List of Figures

List of Tables

1 Introduction

The solution to some underwater acoustics problems requires the use of highly directive sound beams. If the solution further requires that the frequency of the sound be low and that the source size be small, then the sonar designer is faced with quite a challenge. This is because, in conventional sound source designs, increased directivity is achieved through increased source size. In this Technical Memorandum, we discuss the design of a nonconventional sound source that is physically small yet able to produce highly directive, low frequency sound beams. The source relies on the principles of nonlinear acoustics and is called the parametric array.

In a review of the history of nonlinear acoustics [1], Blackstock traces the idea that acoustic wave equations might be nonlinear back to the days of Euler and Lagrange in about 1760 [2,3]. In a review of the applications of nonlinear acoustics, Hamilton points out that it has only been during the past thirty years that people began to apply nonlinear acoustic phenomena [4]. The period started in about 1960 with Peter Westervelt's invention of the parametric array [5]. It was, however, Berktay's discussions of applications of parametric arrays that prompted the interest of the underwater acoustics community, and by the end of the 1960's approximately one hundred papers a year were being written on parametric sonars [6,7].

This Technical Memorandum is divided into six sections: The first is this introduction. The second section is a non-mathematical overview of the basics of nonlinear acoustics. This section is primarily intended for people who are not familiar with either nonlinear acoustics or parametric arrays. The third section is a very brief review of the source level and directivity of a piston source as developed using linear theory. The results of this section are later contrasted with the results of the parametric array. In the fourth section, we present relations that govern the beamwidth and source level of the difference frequency generated by a parametric array which is linear absorption limited in the collimated zone near the source. Methods of estimating the beamwidth and source level when this is not the case are also pointed out. The fifth section contains a design proposal for a parametric array that is referred to as the line-in-cone type. Three different lines of ceramic rings are proposed for the same cone. Performance predictions for the first line indicate a useful frequency range of 0.86–20 kHz with, respectively, source levels of 171–222 dB//1μPa and 3 dB beamwidths of 10.0°–2.3°. Performance predictions for the second line indicate a useful frequency range of 0.30–10 kHz with, respectively, source levels of 170–219 dB//1μPa and 3 dB beamwidths of 8.6°–2.9°. The third line should have a useful frequency range of 0.15–5 kHz with, respectively, source levels of 170.5–212 dB//1μPa and 3 dB beamwidths of 7.6°–4.8°. The strength of the design is its simplicity that results in a low cost of construction. Its disadvantages are also discussed. The final section of this Technical Memorandum is a summary.

2 Overview of Nonlinear Acoustics and Parametric Arrays

This overview is intended to introduce the non-specialist to the basic concepts of nonlinear acoustic wave propagation without the use of mathematics. We first review how and why acoustic waves steepen (distort) and form shocks. This is examined in both the time and frequency domains. We then discuss the effects of thermoviscous attenuation and show the role

that they play in acoustic saturation. Finally, we review the operation of a parametric array.

Let us now define some nomenclature. Throughout this discussion, the words small-signal and linear theory are used interchangeably; the words finite-amplitude and nonlinear theory are also used interchangeably. The reason is that the standard acoustic theory that people are familiar with is a linear theory. It is obtained by assuming that the acoustic signal is infinitesimally small—hence small-signal means linear theory. On the other hand, if the acoustic signal is no longer infinitesimally small, but is of finite-amplitude, the governing equations are nonlinear—thus finite-amplitude means nonlinear theory.

Because the basic concepts of nonlinear acoustics are sometimes difficult to understand, we start by considering a rather crude analogy: a water wave approaching a beach. As the wave nears the beach, the wave begins to distort, and the front face of the wave begins to steepen. This phenomena arises because the water at the top or peak of the wave is travelling faster than the water at the base or trough of the wave. Soon the wave forms a vertical wall, a discontinuity. The water wave then does something that the sound wave cannot do—it breaks. Sound waves do not break, but sound waves can steepen and form discontinuities. A discontinuity in a sound wave is referred to as a shock, and shock formation is one of the central phenomena in nonlinear acoustics.

The reason that an acoustic wave steepens and forms a shock is the same as that for a water wave: The propagation speed of all points on the wave is not constant. The factors that contribute to the non-constant propagation speed of an acoustic wave are, first, convection: The motion of the fluid particles themselves is contributing to the propagation speed. The second factor is the nonlinear relation between the pressure and the density. The combined magnitude of both effects is given by a nondimensional number called the coefficient of nonlinearity β, which for water is about 3.5. It turns out that the relation for the propagation speed of a wavelet on a plane wave is

$$\frac{dx}{dt} = c_0(1 + \beta \frac{u}{c_0}) \quad ,$$

where a wavelet is any specific point on a wave, c_0 is the small-signal sound speed (the value tabulated in standard texts), and u is the acoustic particle velocity [8].

Much may be gained from an examination of the propagation speed relation. The propagation speed relation implies something about the rate at which waves steepen and form shocks. The bigger the amplitude (u/c_0), the faster the wavelet propagates; the faster the wavelet propagates, the sooner that the wave steepens and forms a shock. Accordingly, one may infer from the propagation speed relation that, to achieve the same amount of nonlinear steepening, waves of small amplitude must propagate much further than waves of large amplitude. For example, plane waves with the amplitude of ordinary speech ($u/c_0 \simeq 10^{-7}$) must propagate ten thousand times further than plane waves with the amplitude of jet engine noise ($u/c_0 \simeq 10^{-3}$). The propagation speed relation also implies that any wave, regardless of amplitude or frequency, will eventually steepen and form a shock. This leads one to question why linear acoustics works so well and why we do not routinely observe shock formation. Simply stated, the reason is that we have neglected thermoviscous attenuation. The energy in small-signal waves, such as ordinary speech, is absorbed before any appreciable amount of nonlinear steepening occurs.

Our discussion of nonlinear steepening and shock formation has, until now, been based on

the idea that an acoustic wave changes its shape as it propagates. This is, accordingly, a time domain analysis procedure and may be used to study waves of arbitrary shape. We now restrict ourselves to waves with a harmonic source excitation (called the primary) and use frequency domain (Fourier) analysis to aid our understanding. Recall our water wave analogy and the fact that the wave steepened and eventually formed a shock. As you can imagine, the Fourier decomposition of a shock is rich in harmonics. Thus it is reasonable to assume that the process of nonlinear steeping is a process that takes energy out of the primary and puts it in the higher harmonics. The generation of higher harmonics is sometimes referred to as the self-action of the wave. The term implies that the wave is acting on itself to generate the higher harmonics.

It turns out that the nonlinear conversion of energy from the primary to the higher harmonics leads to another phenomenon—acoustic saturation. Once saturation is fully developed, one witnesses no increase in the received sound pressure level (SPL) of the primary despite increases in its transmitted SPL. To understand why saturation occurs, first recall that the thermoviscous attenuation of the fluid increases with frequency squared. Second recall that the higher the source amplitude, the sooner nonlinear steepening occurs, and hence the sooner nonlinear conversion of energy from the primary to the higher harmonics occurs. Since the higher harmonics are attenuated at a faster rate, the wave energy is absorbed sooner. Thus the increased amplitude leads to an increased rate of absorption. It is this no-win situation that ultimately limits the source level of the parametric array.

So far we have learned that the propagation speed of all points on a wave is not constant. Nonlinear phenomena that are a direct consequence of the non-constant propagation speed are, in the time domain, waveform steepening and the formation of shocks or, in the frequency domain, the shifting of energy from one frequency to higher frequencies. We have also seen that the upshifting of energy from the primary to higher harmonics, where attenuation is higher, eventually leads to saturation.

Now suppose that two pure tones are present at the source. We call these two tones the primaries. With our current knowledge, we expect that the self-action of each primary will generate its own set of higher harmonics. It turns out that a nonlinear interaction also takes place between the two primaries. The interaction does not take place at the source, but takes place throughout the fluid. If the source is, say, a piston, then the zone of interaction is confined to the narrow, main lobe of the beampattern generated by the piston. The zone of interaction is, however, quite long and is sometimes referred to as a virtual array of sources. In the virtual array, the self-action of the two primaries is generating their higher harmonics. Simultaneously, the interaction between the two primaries is generating signals with frequencies equal to the the sum of and the difference between the two primaries, which we refer to as the sum and difference frequencies.

Now suppose further that the frequencies of the two primaries are very high, say, about 30 kHz and differ by only, say, 2 kHz. Thermoviscous absorption in the fluid acts as a natural low-pass filter that absorbs the two high frequency primaries and all of the higher harmonics. Thus all that is left is the difference-frequency signal generated by the nonlinear interaction between the two primaries throughout that long, narrow zone of interaction. This is a parametric array, a device that results in a narrow beam of low frequency sound from a small source.

A further benefit of a parametric array is that the difference frequency radiation pattern

has almost no sidelobes. The reason that sidelobes are so low is that the virtual array of sources acts, approximately, as an exponentially tapered end-fire array. The taper is caused by the natural thermoviscous absorption of the fluid.

Although parametric arrays can result in dramatic improvements over what you would get using the same size source in a linear fashion, they are not a panacea. They are very inefficient. Only a small fraction of the energy in the primaries is shifted to the difference frequency. However, if you are working in a highly reverberant environment and you only want to ensonify a particular direction, then a parametric array may be just what you want.

To improve the directivity of the parametric array, we should lengthen the zone of interaction. One way of doing this is to lower the primary frequency to decrease primary attenuation. The problem with this is that a lower primary frequency requires a larger source, and a small source size is one of the principle attractions of a parametric array. Thus the design of a parametric array is a series of compromises between source size, primary frequency, difference-frequency directivity, and difference-frequency source level. One of the purposes of the following sections is to quantify how these parameters interrelate.

3 Piston Directivity using Linear Acoustics

We now briefly examine the source directivity of a piston source as derived using standard linear acoustic theory. We later contrast these results with the results for the difference frequency generated by a parametric array. To achieve a narrow (4° between 3 dB down points) beam of 2000 Hz sound using a conventional source, we would require a circular piston with a radius of 5.54 m. Similar results will be obtained using other (non-circular) piston shapes.

The calculation of the required piston area is simple and demonstrates that, to achieve directivity in a conventional (non-superdirective) source using linear theory, almost no alternative to source size exists. The acoustic pressure p in the farfield of a circular piston of radius a that is vibrating with angular frequency ω is as follows [9]:

$$p(r,\theta,t) = j\frac{p_0 r_0}{r} D(\theta) e^{j(\omega t - kr)} \quad , \tag{3.1}$$

where r is the range from the center of the piston, θ is the angle from the axis of symmetry of the piston, t is the time, $k \equiv \omega/c_0$ is the acoustic wavenumber, and j is $\sqrt{-1}$. The peak pressure on the face of the piston is p_0 and is approximately equal to $\rho_0 c_0 u_0$, where ρ_0 is the static density, c_0 is, as above, the small-signal sound speed, and u_0 is the peak velocity of the piston. The Rayleigh distance is $r_0 \equiv S_0/\lambda$, where S_0 is the area of the piston face and λ is the acoustic wavelength. (Note that for a circular piston, the Rayleigh distance may be expressed as $ka^2/2$.) The directivity factor $D(\theta)$ is defined as follows:

$$D(\theta) \equiv \frac{2J_1(ka\sin(\theta))}{ka\sin(\theta)} \quad , \tag{3.2}$$

where J_1 is the first-order Bessel function. Note that the directivity factor exhibits oscillations (sidelobes) that decay with increased $ka\sin(\theta)$. The level of the first (largest) sidelobe relative to the mainlobe is -17.5 dB. Examining the mainlobe we see that, at the half power points,

the directivity function has the value $1/\sqrt{2}$. This implies that the half power beamwidth of the circular piston is given by

$$ka \sin \theta_{HP} \simeq 1.62 \quad . \tag{3.3}$$

Thus, if the frequency of interest and the beamwidth desired are known, the value of the radius a is effectively specified as well. Accordingly, we conclude that to achieve source directivity with a circular piston (which is typical of many sources designed using linear acoustic theory), there is no linear (non-superdirective) alternative to source size.

Some final comments: Note that according to Eq. (3.1), the source level of the piston $p_0 r_0$ may be increased by increasing the piston velocity (displacement) with no limit. Moreover, Eq. (3.3) indicates that the increase in source level has no effect on beamwidth. These observations are not true indefinitely, and they do not apply to parametric arrays, as we shall soon see.

4 Source Level and Directivity of Difference Frequency from a Parametric Array

4.1 Introduction

Precise performance prediction of parametric arrays is difficult because one must account for the combined effects of thermoviscous absorption, nonlinear attenuation (harmonic generation and losses), geometric spreading, as well as beam diffraction. This level of performance prediction is not, as yet, available at DREA, although computer models developed by Tjøtta and Tjøtta may be obtained [10]. Meanwhile, the performance curves developed by Moffett, Mellen, and Konrad are the most accurate information that is readily usable [11,12,13,14,15]. The curves give estimates of the difference-frequency source level and the difference-frequency beamwidth. (The difference-frequency beamwidth is expressed in terms of a decrease in the directivity index relative to the directivity index of the primary frequency.) These design curves are used to predict the performance of the design proposed in the next section.

The purpose of this section is to provide the reader with a basic understanding of the trade-offs between source size, the ratio of primary to difference frequency, and the difference-frequency beamwidth or source level. To do this we present some equations that, unlike the design curves, are not valid for all situations. The reason for using the equations is that they do a better job of providing a basic understanding of the operation of a parametric array than the design curves do.

The reason that the equations have a limited range of validity is that they are derived assuming that all the interaction between the two primaries occurs in the collimated zone near the source. In other words, the equations are derived assuming that the primaries are effectively dissipated by linear absorption in this zone. This assumption and its implications are quantified later in this section. For now it is sufficient to note that the assumption is usually violated by parametric arrays designed for ocean acoustics use because ocean acoustics requires high difference-frequency source levels. The requirement causes sonar designers to increase the primary source level to the point at which the primaries form shocks in the nearfield, thereby

violating the assumption of linear absorption in the nearfield. For more details, see, for example, the introduction in reference [12].

A second assumption that underlies the derivation of the equations presented is that the primary beamwidth be at least as narrow as the desired difference-frequency beamwidth. This assumption constrains both the choice of primary frequency and the size of the source: If a lower primary frequency is desired, a larger source is required or else the difference-frequency beamwidth increases.

It turns out that for the purpose of calculations of beamwidths and source levels of a parametric sonar, estimates of sound absorption in seawater are required. To obtain these estimates, we used the relations developed by Fisher and Simmons [16] as presented in the book by Kinsler *et al.* [9]. The temperature is assumed to be 5°C, the salinity 35 ppt, and the pH 8.0. We then linearized the region between 10 kHz and 20 kHz to develop the following approximate relation:

$$\overline{\alpha} = 6.85 \times 10^{-12} f^2 + 0.1265 \times 10^{-3} \quad \text{dB/m} \quad , \tag{4.1}$$

where f is the frequency in Hz, and α and $\overline{\alpha}$ are related by

$$\alpha = \overline{\alpha}/8.686 \quad \text{nepers/m} \quad . \tag{4.2}$$

Equation (4.1) is a reasonable estimate of the sound absorption in the 7–40 kHz region and will be used for all sound absorption calculations.

4.2 Difference-frequency beamwidth

Making all the assumptions stated above, Berktay conducted an analysis of the parametric array and derived relations for the source level and directivity [6]. The source level is discussed in the next section. Berktay's result for the directivity is

$$D_d(\theta) = \frac{2J_1(ka\sin(\theta))}{ka\sin(\theta)} \left\{ 1 + \left[\frac{2\kappa_d}{\alpha_T} \sin^2(\theta/2) \right]^2 \right\}^{-1/2} \quad , \tag{4.3}$$

where $k_d \equiv \omega_d/c_0$ is the wavenumber of the difference-frequency sound and $\alpha_T \equiv \alpha_1 + \alpha_2 - \alpha_d \cos\theta$ (nepers/meter) is the composite attenuation, α_1 is the attenuation coefficient of the 1st primary, α_2 is the attenuation coefficient of the 2nd primary, and α_d is the attenuation coefficient of the difference frequency. In his discussion of this result, Berktay notes that the directivity pattern of the parametric array is the product of the directivity caused by the finite cross section of the collimated beam and the directivity of the exponentially tapered end-fire array of virtual sources. More significant to our discussion is Berktay's observation that the directivity pattern has only one lobe, that is, a main lobe with no sidelobes. Although Berktay's analysis is set upon the assumptions stated above, a later and more detailed analysis conducted by Moffett and Mellen only slightly modifies this conclusion [11,12]. The absence of sidelobes is a noticeable deviation from the standard linear theory results and is one of the hallmarks of a parametric array.

For a high ka source, Berktay also reduced his directivity pattern result to the following relation for the 3 dB down beamwidth of difference-frequency sound generated by a parametric

array:

$$\theta_{3\,\mathrm{dB}} = 4\sqrt{\frac{\alpha_T}{2k_d}} \quad . \tag{4.4}$$

Equation (4.4) is markedly different from the small-signal relation governing the beamwidth of a circular piston, Eq. (3.3). Most striking is the dependence on the fluid absorption. The explanation for this is as follows: The faster the primary frequency is absorbed, the shorter the length of interaction zone becomes, and hence the difference-frequency beam widens. This idea is reflected in Eq. (4.4). Noting that the fluid absorption approximately increases in proportion to the square of the primary frequency, we see that, if the difference frequency is held constant, the difference-frequency beamwidth increases with primary frequency. Thus, narrower beams may be achieved by using lower primary frequencies. As noted earlier, however, the lower the primary frequency, the larger the source must become.

4.3 Difference-frequency source level

For a parametric source with circular primary drivers and which is linear absorption limited in the primary nearfield, the difference-frequency pressure in the farfield ($r \gg r_0, 1/\alpha_T$) is given by the following [6]:

$$p_d = \frac{\beta\omega_d^2 p_1 p_2 S_0 e^{-\alpha_d r}}{4\pi\rho_0 c_0^4 \alpha_T r} \quad . \tag{4.5}$$

At an effective range of 1m, and using the values of $c_0 = 1500$ m/s, $\rho_0 = 1000$ kg/m^3, and $\beta = 3.5$, Eq. (4.5) becomes (after converting the relation to dB)

$$SL_d - SL_1 = -292.8 - 20\log(\alpha_1 r_0) + 40\log\left(\frac{f_d}{f_1}\right) + SL_1^* \quad , \tag{4.6}$$

where $SL_d = 20\log(p_d) + 117$ is the source level of the difference frequency, $SL_1 = 20\log(p_1 r_0) + 117$ is the on-axis source level of the circular piston primary, and SL_1^* is the frequency-scaled source level of the primary,

$$SL_1^* = SL_1 + 20\log\left(\frac{f_1}{1000}\right) \quad . \tag{4.7}$$

Equation (4.6) shows that to achieve the maximum difference-frequency source level, we may do any or all of the following: (1) increase f_d/f_1 until it approaches its limit, unity; (2) decrease $\alpha_1 r_0$, which is usually much less than unity, and (3) increase SL_1. As noted above, these actions must be moderated by the requirement for a highly directive primary beam, which implies a large source or high primary frequency.

4.4 Range of validity

Equations (4.4) and (4.6) are valid as long as the primaries are absorbed by linear absorption in the collimated zone near the source. The length of the collimated zone near a source is approximately equal to the Rayleigh distance, r_0. A requirement to satisfy the assumption that the primary be *linearly* absorbed in the collimation zone is that no shocks form in the collimation

zone. Thus the shock formation distance of the collimated primary $\rho_0 c_0^3/2\pi\beta p_1 f_1$ must be much greater that the collimation length,

$$\frac{\rho_0 c_0^3}{2\pi\beta p_1 r_0 f_1} \gg 1 \quad . \tag{4.8}$$

To satisfy our assumption that the primary be absorbed in the collimation zone, we see that the length of the collimation zone must be much greater than the linear absorption length of the parametric array, $1/\alpha_T$. This requirement may, however, be relaxed slightly. Mellen and Moffett have shown that the primary beam may be treated as a collimated beam as long as all the nonlinear interaction occurs well before the distance, $f_1 r_0/f_d$ [12]. Thus, this linear absorption requirement is

$$\alpha_T r_0 \frac{f_1}{f_d} \gg 1 \quad . \tag{4.9}$$

As was noted earlier, it turns out that both of these requirements are violated by many parametric arrays designed for ocean acoustic use. For any situation in which either of the above requirements is violated, Eqs. (4.4) and (4.6) may not be used. The designer must then use the design curves of Mellen and Moffett to obtain estimates of $SL_d - SL_1$ and 3 dB beamwidth [12,15].

Examples of Mellen and Moffett's parametric array design curves are shown in Figs. 1 and 2. The curves in Fig. 1 give the difference-frequency source level relative to the primary source level ($SL_d - SL_1$) as a function of the frequency-scaled primary source level (SL_1^*) at $\overline{\alpha}_1 r_0 = 0.1$ dB for a range of parametric step-down ratios (f_1/f_d = 3–500). For other values of $\overline{\alpha}_1 r_0$, refer to Ref. [15]. The curves in Fig. 2 give the change in directive index (DI) of the difference-frequency beam relative to the directive index of a primary beam as a function of the frequency-scaled primary source level (SL_1^*) at $\overline{\alpha}_1 r_0 = 0.1$ dB for the same range of parametric step-down ratios. Figure 1 gives us the same information as Eq. (4.6), but is valid over a wider range of primary source levels, primary frequencies, etc. Similarly, Fig. 2 effectively gives the same information as Eq. (4.4), but one must calculate the beamwidth knowing the primary DI. Inspection of the difference-frequency source level curve in Fig. 1 clearly shows that increased primary source level does not always result in an increased difference-frequency source level. Moreover, the design curves for the change in the difference-frequency directivity index show that increasing the source level almost never results in an increase in directivity and may in fact decrease the directivity. Figures 1 and 2 are used in the next section to design a parametric array.

5 Design Proposal for a Parametric Array

It is interesting to consider a simple and relatively inexpensive design for a parametric array. The proposed design is called the *line-in-cone* type because the drivers are an interchangeable line of piezoelectric cylinders that radiate radially. The line of drivers is located on the axis of symmetry of a 45° cone that reflects the cylindrically propagating energy from the line into the forward direction. See Fig. 3. The line-in-cone design is not new and has been used many times in the past at Applied Research Laboratories: The University of Texas at Austin and

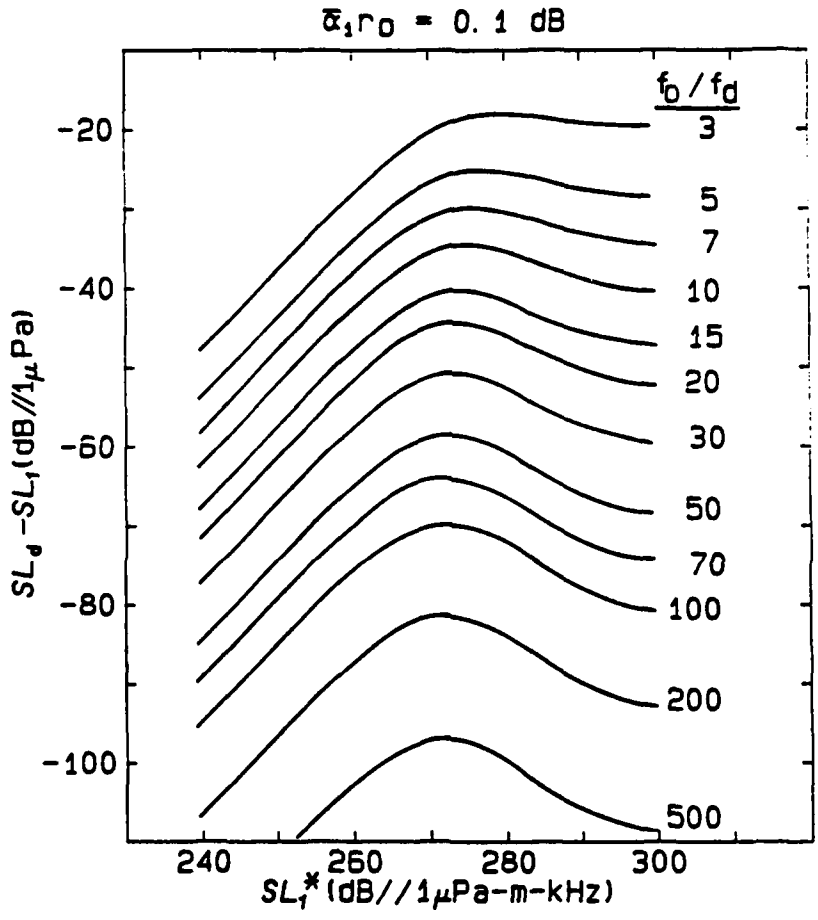

Figure 1: *Design curves giving the difference-frequency source level relative to the primary source level ($SL_d - SL_1$) as a function of the frequency-scaled primary source level (SL_1^*) for a range of parametric step-down ratios (f_1 / f_d) assuming a single value of fluid absorption and Rayleigh distance, $\bar{\alpha} r_0 = 0.1$.*

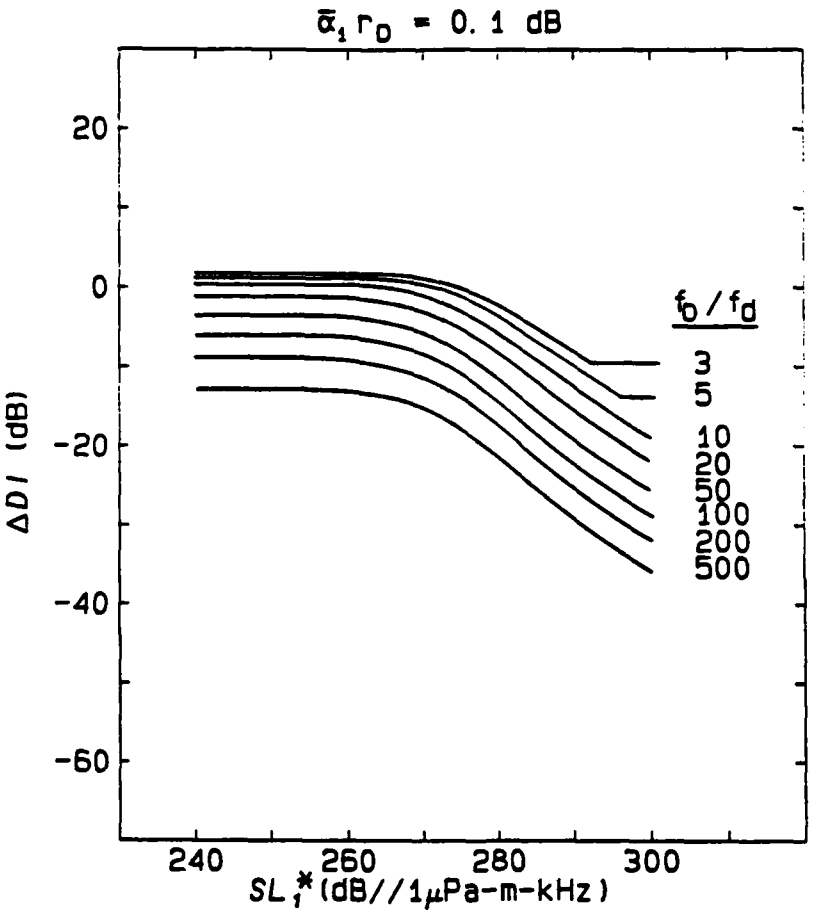

Figure 2: *Design curves giving the change in directive index (DI) of the difference-frequency sound relative to the directive index of the primary beam as a function of the frequency-scaled primary source level (SL_1^*) for a range of parametric step-down ratios (f_1 / f_d) assuming a single value of fluid absorption and Rayleigh distance, $\bar{\alpha} r_0 = 0.1$.*

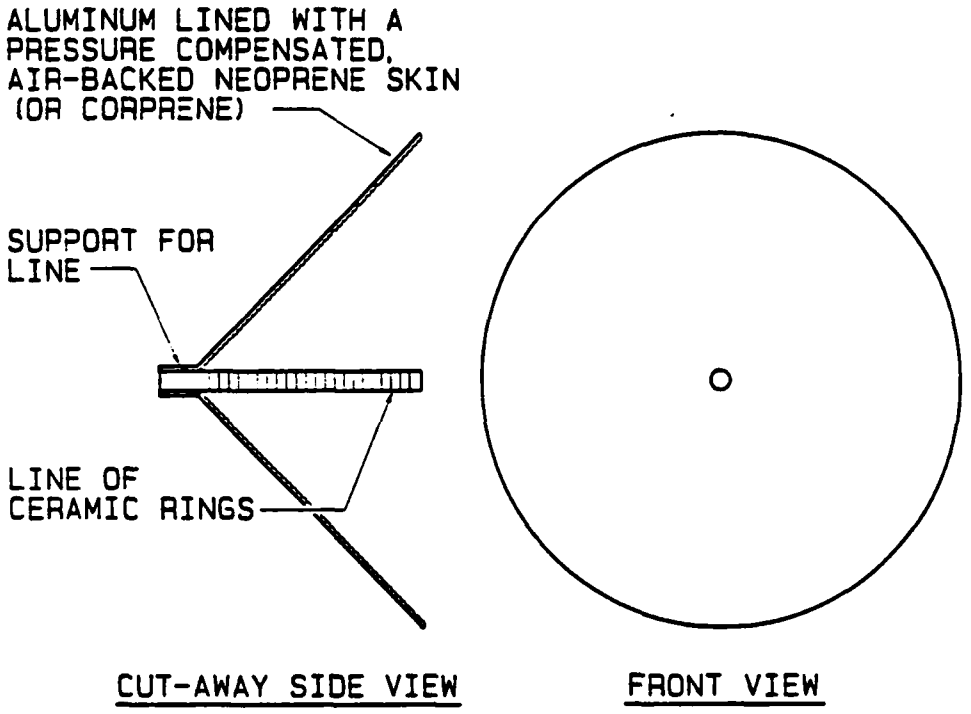

Figure 3: *Sketch of the line-in-cone type parametric source*

elsewhere.[1] What is new is the proposed modification to the ring suspension (not potted), the proposed ability to interchange lines in the same reflector cone, and the air-backed, pressure compensated reflector surface.

An alternative parametric array design that has the advantage of electrical beam-steering is to use an array of small (Tonpilz) piston drivers. Anytime that rapid angular sweeps are required, the electrically steered array is the preferred choice. However, if rapid sweeps are not required, the line-in-cone design should suffice. Moreover, the many small drivers and the precision machining required to hold the drivers is likely to cost more than the line-in-cone. The line-in-cone approach uses banded ceramic rings (approximately US $4000 total) and a reflector baffle, which need not be precisely manufactured. The substantial electrical amplifier requirement for both designs is about the same. The other issue regarding the control of beam-steering—be it mechanical or electrical—has not been addressed.

[1] For example, a line-in-cone cone design was used by DREA as a receiver in volume reverberation experiments around 1970 [17,18].

The remainder of this section proceeds as follows: We first address the basic design of the source, which is independent of the primary frequency and source size. We next discuss the choice of primary frequency and source size. Following that we choose a line of piezoelectric rings and discuss the primary source level, which includes the effects of directive gain. The electrical power requirement is then examined. Next we address the most interesting part—the predicted difference-frequency source level and beamwidth. Finally we consider two other lines of piezoelectric rings that may be inserted into the same reflector and give performance predictions using them. These lines are not required to meet the design goals (outlined below), but help demonstrate the flexibility of the line-in-cone design.

5.1 Construction of the line and reflector

The reflector shown in Fig. 3 is to be lined with corprene, a cork-like material, to achieve a pressure-release boundary at shallow depths. For deeper depth operation, an air-backed, pressure compensated, neoprene skin would have to be used. A pressure-release reflection is preferred over a rigid-wall reflection for three reasons: (1) Weight: An acoustically soft (relative to water) material such as cork is usually much lighter in weight than an acoustically hard material such as steel. This results in ease of handling. Moreover, since the acoustic impedance of water is moderately high at 1.54×10^6 MKS rayls, it is relatively easy to find materials that have acoustic impedances that are much smaller (softer) than that of water. (2) Upon reflection from a rigid wall, the peak pressure *at the wall* approximately doubles. This may cause cavitation at the wall and thereby dramatically decrease the performance of the source. On the other hand, upon reflection from a pressure release boundary, the pressure at the boundary is zero. (3) It turns out that, because of the 180° phase shift, the pressure-release reflection will *undo* the nonlinear distortion that occurs between emission from the line of ceramic rings and the wall [19]. This will result in a longer interaction zone; that is, it increases the length of the virtual array and thereby improves directivity.

The suspension system for piezoelectric ceramic ring elements in the line-in-cone source is shown in Fig. 4 and is the result of a conversation with G. W. McMahon of DREA. The rings are suspended between three brass rods in an oil-filled clear plastic tube. The rods are terminated in fiberglass endpieces that serve as the caps for the tube. One or two other fiberglass supports may be required along the length of the tube. The ceramic rings are suspended from the rods by rubber (neoprene) bands that are tied to the rods with string. In this way individual elements may be replaced without complete disassembly. The brass rods also serve as the conductors, one at f_1, one at f_2, and one common. The short electrical leads with a single loose loop from the rods to each ring provide the electrical power. The rings are to be banded so that they may be tangentially driven. Moreover, they are wired for parallel operation in their centres. All electrical connections are to be bonded on for mechanical rigidity.

5.2 Primary frequencies and source size

It is assumed that the maximum source dimension is to be about 1 m and that the maximum difference-frequency beamwidth is to be about 4° between the 3 dB down points. The desired range of difference frequencies is 1–10 kHz. We therefore seemingly arbitrarily state that the

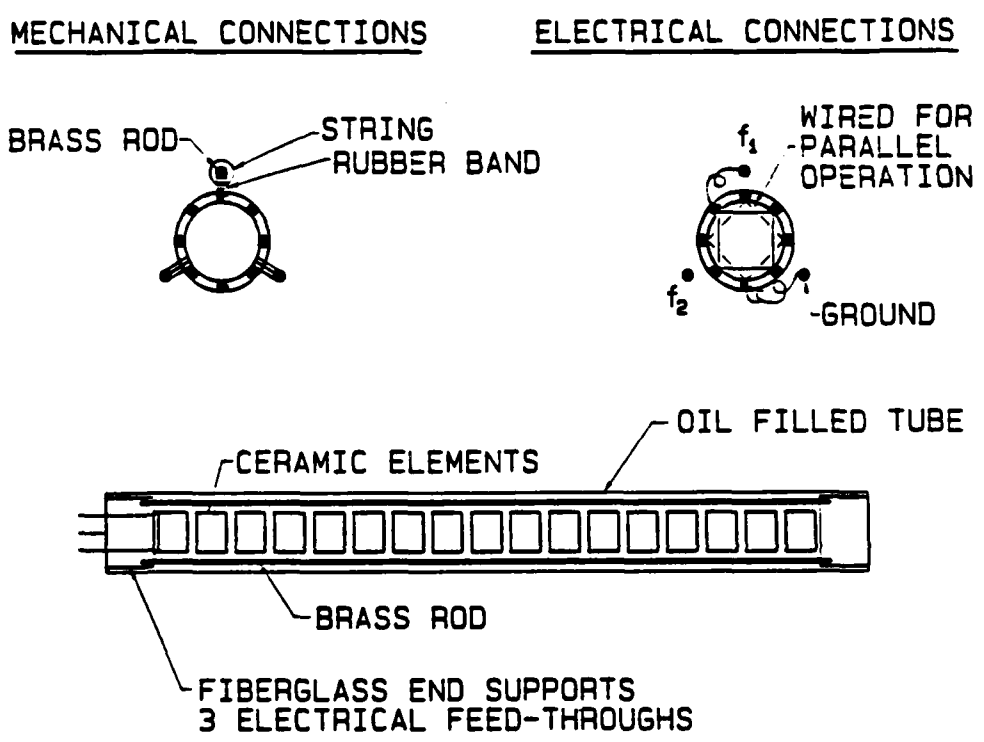

Figure 4: *Sketch of the suspension of piezoelectric ceramic ring elements for line-in-cone source*

diameter of the reflector is 1.1 m and that the area of the reflector's mouth is 0.95 m^2. If the face of the reflector is assumed to act like a piston, Eq. (3.3) may be used to calculate the minimum primary frequency of about 20 kHz. Since the difference between the two primaries is to be as large as 10 kHz, we choose 30 kHz as the nominal primary frequency.

5.3 Primary source level

The source level of the line of rings is now addressed. Because the primary frequencies are in the 20–35 kHz region, the results of a free-flooding ring study by McMahon may be used [20]. The rings have an inner radius of 1.59 cm, a wall thickness of 0.32 cm, and a length of 1.21 cm. Thus the number of rings that it takes to fill the axial line is 36 (allowing for a 3 mm gap between each ring). If the 36 rings are alternately driven at f_1 and f_2, each primary frequency is driven on 18 rings. According to McMahon's results, we should have no difficulty achieving a level of 33 μbar/V@1 yd from each ring when driving the ring radially.[2] This results in 129.6 dB//1μPa@1 m from each ring with 1 V applied. With an applied voltage of 960 V (3000 V/cm) and a *DI* of 2 dB, we have 44.1 acoustic watts per ring. The total acoustic power for the 18 element line is 794 W. This estimate assumes the rings are polarized radially. If the rings are polarized tangentially, an additional 6 dB of output can be obtained.

To improve our estimate of the signal level at the mouth of the reflector, we can examine the interaction at the reflector. We first examine the sea water–cork interface and find that the reflection coefficient at 45° is −0.893, or a reflection loss of about 1 dB.[3] Going from the sea water into the cork, no critical angle exists. The proposed cork layer is to be backed by aluminum. The critical angle from cork into aluminum is 5.6°, and the incoming energy is entirely reflected. (There is a phase shift, but that is not important here.) The transmission coefficient from the cork back into the sea water is 1.893, and, accordingly, the pressure wave that was initially transmitted into the cork re-enters the water with amplitude of 0.203. If this wave were 180° out of phase with the reflected wave, then the loss might be as high as −3.2 dB upon reflection. Noting this, the hard steel reflector appears to be a better choice. The sea-water interface with steel has a critical angle of 17.3°, and the reflection coefficient at normal incidence is 0.924, which yields a reflection loss of 0.7 dB. In the long run, however, the air-backed system offers the best solution with a reflection coefficient of −0.9997. For reference, the sea water–aluminum interface has a critical angle of 16.9°, and a normal incidence reflection coefficient of 0.80. For purposes of our calculations, we use the value of the cork reflector, −1 dB.

The presence of the reflector affords us considerable directive gain. At 30 kHz, the reflector is 22λ in diameter at the mouth. Assuming that the sound at the mouth of the reflector acts as a uniform piston in an infinite baffle, we obtain the directivity index of the reflector, 36.8 dB. Note that we have neglected the inherent amplitude shading that occurs with the line-in-cone device in calculating the directivity index.

[2]This is not the peak value in McMahon's results, but the peak value relies on both the ring and cavity modes. In our case however, the cavity mode will probably not contribute because of the close placement of the rings.

[3]This and the future calculations are based on the values from the book by Kinsler *et al* [9]: cork: c_0 = 500 m/s, ρ_0 = 240 kg/m^3, Z = 0.12 × 10^6 MKS rayls; 13°C sea water: c_0 = 1500 m/s, ρ_0 = 1026 kg/m^3, Z = 13.9 × 10^6 MKS rayls; aluminum: c_0 = 5150 m/s, ρ_0 = 2700 kg/m^3, Z = 13.9 × 10^6 MKS rayls; and steel: c_0 = 5050 m/s, ρ_0 = 7700 kg/m^3, Z = 39.0 × 10^6 MKS rayls.

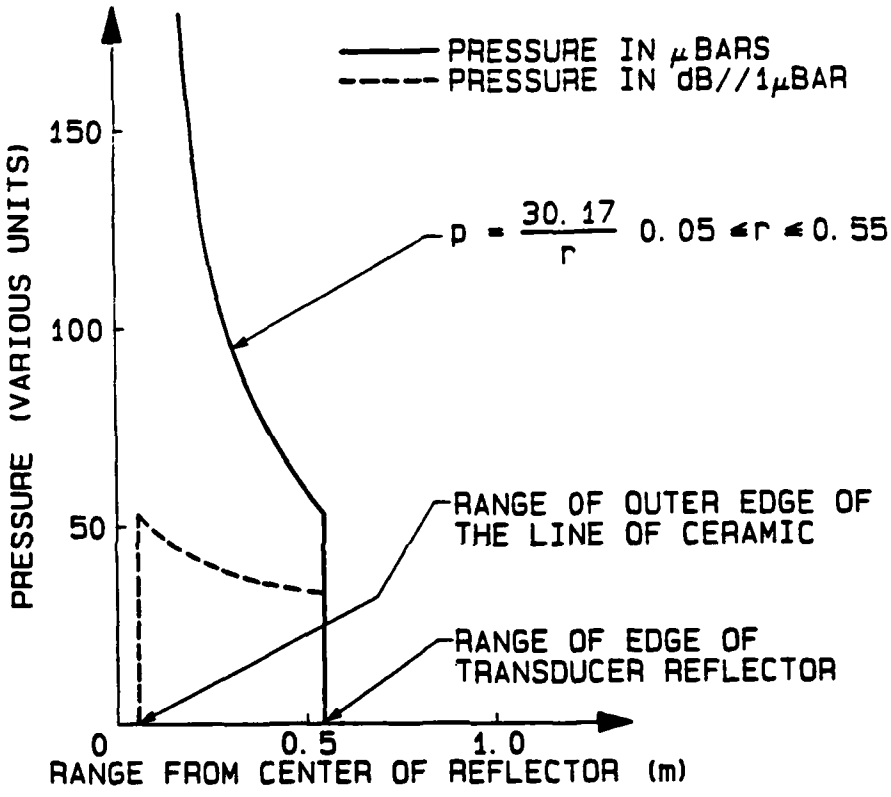

Figure 5: *Sketch of the pressure distribution across mouth of line-in-cone reflector.*

We now calculate a correction for the amplitude shading. Since the sound propagating away from the line of ceramic rings does so in a cylindrical fashion, the pressure distribution at the mouth of the reflector has a $1/r$ shape. Assuming that the line of ceramic cylinders provides uniform excitation, we expect the pressure distribution to have the form shown in Fig. 5. Because of nonlinearity, losses upon reflection, ceramic element interaction, etc., it is somewhat unlikely that the actual pressure distribution will be as shown in Fig. 5; it is, however, a reasonable estimate.

We use the pressure distribution in Fig. 5 to calculate the directivity index of the reflector from first principles. Recall that the directivity index is defined as follows [9]:

$$DI \equiv 10\log\left[\frac{4\pi}{\int_0^{4\pi}[D(\theta,\phi)]^2 d\Omega}\right] \quad , \tag{5.1}$$

where θ and ϕ are the spherical coordinate angles, $d\Omega$ is a element of solid angle, and $D(\theta,\phi)$ is the pressure directivity function. For cylindrically symmetric objects such as circular pistons, the pressure directivity function is defined as

$$D(\theta) \equiv \frac{p(r,\theta,t)}{p(r,0^\circ,t)} \quad . \tag{5.2}$$

To obtain an estimate of $p(r,\theta,t)$, we must *re-do* the piston problem. The differences between this derivation and the standard textbook version are (1) the different limits of integration and (2) the non-uniform particle velocity distribution. Following Morse [21], we see (as shown in Fig. 6) that the element of pressure dp contributed by the element of the piston face ds is

$$dp \simeq j\frac{\rho_0 c_0 k}{2\pi r} u e^{j(\omega t - kr)} e^{jky\sin\theta\cos\phi} y\, dy\, d\phi \quad . \tag{5.3}$$

Noting that u is a function of y that must be included in the integral leads to the following:

$$p(r,\theta,t) = j\frac{\rho_0 c_0 k}{2\pi r} e^{j(\omega t - kr)} \int_b^a uy\, dy \int_0^{4\pi} e^{jky\sin\theta\cos\phi} d\phi \quad . \tag{5.4}$$

The integral over y results in $2\pi J_0(ky\sin\theta)$. Re-writing the non-uniform particle velocity u as u_0/y yields

$$p(r,\theta,t) = j\frac{\rho_0 c_0 k}{r} u_0 e^{j(\omega t - kr)} \int_b^a J_0(ky\sin\theta)\, dy \quad . \tag{5.5}$$

Use of Eq. (5.5) in Eq. (5.2) results in

$$D(\theta) = \frac{\int_b^a J_0(ky\sin\theta)\, dy}{a-b} \quad , \tag{5.6}$$

where the denominator is obtained by applying the $\theta = 0^\circ$ condition before the integration. The DI is then calculated by using Eq. (5.6) in Eq. (5.1)

$$DI = 10\log\left\{\frac{4\pi}{2\pi\left(\frac{1}{a-b}\right)^2 \int_0^{\pi/2}\left[\int_b^a J_0(ky\sin\theta)\, dy\right]^2 \sin\theta\, d\theta}\right\} \quad . \tag{5.7}$$

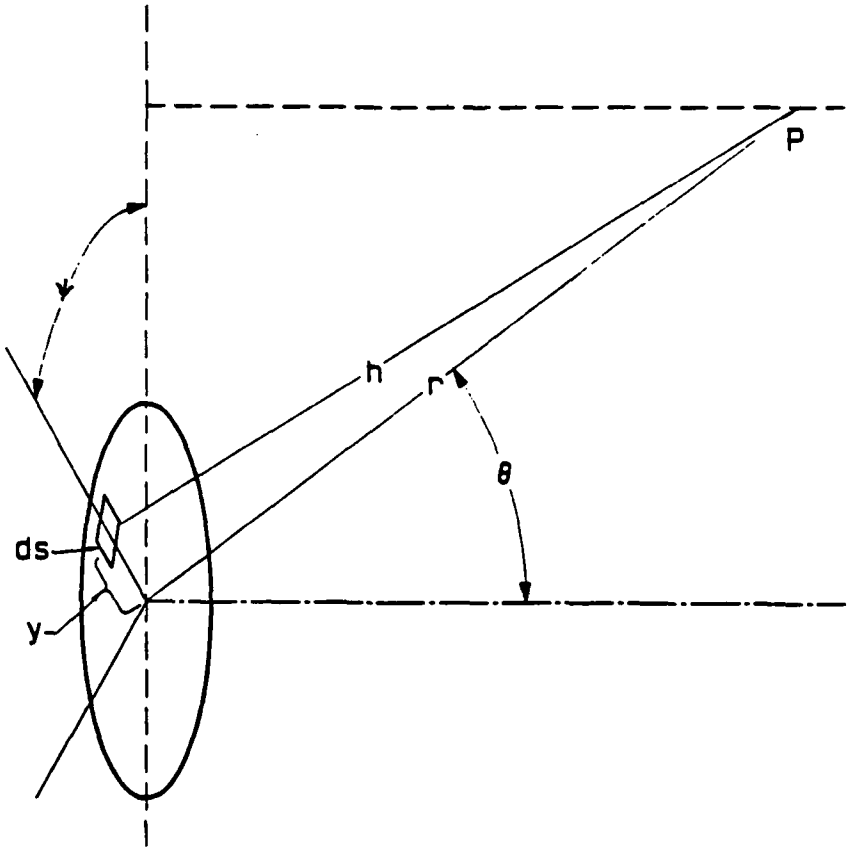

Figure 6: *Sketch of geometry of piston problem (after Morse [21]).*

This integral was evaluated numerically using *Mathematica*, and yielded a DI of 35.2 dB. Thus the correction factor are the non-uniform pressure distribution is 1.6 dB.

Accounting for the directive gain with the non-uniform amplitude shading and for the 1 dB loss at the pressure release surface, we calculate the source level as follows: $SL = 10\log(3175) - 1 + 35.2 + 170.8 = 240$ dB//1μPa@1 m.

5.4 Amplifier requirement

The electrical power required to drive the line of ceramic rings may be estimated using an electroacoustic efficiency of 50%. McMahon's results indicate efficiencies in the 75% range, but his results took advantage of both the radial and cavity modes. The acoustic watts in the water generated by each of the primaries is ~3.2 kW. Thus the electrical power input required is ~6.5 kW per primary.

5.5 Difference-frequency source level and beamwidth

The difference-frequency source level and beamwidth may now be calculated. At 30 kHz, the attenuation of 5°C seawater is 724×10^{-6} nepers/m (6.29 dB/km). The 1.1 m diameter mouth of the reflector has a Rayleigh distance of 19 m at 30 kHz. According to Eqs. (4.9) and (4.9), we may not use Eq. (4.6) to estimate the difference-frequency source level. We must therefore use the design curves of Mellen and Moffett with $\overline{\alpha}_1 r_0 = 0.12$ and $SL_1^* = 269.5$ dB. Although the design curves presented earlier in Figs. 1 and 2 are for $\overline{\alpha}_1 r_0 = 0.1$ and not $\overline{\alpha}_1 r_0 = 0.12$, we use them because the results are quite similar. Use of these design curves leads to the performance predictions listed in Table 1.

The values listed in Table 1 show that the source level exceeds 194 dB from 1.5–10 kHz with beamwidths from 4.6–2.9°. Thus despite its inefficient operation, the parametric array provides a sizable source level as well as the desirable features of a small source size, a very narrow main beam, no sidelobes, and a broad operating band of 0.3–10 kHz. This combination of features makes the parametric array an extremely useful tool for broadband applications in which narrow beams and moderate source levels are required.

5.6 Performance with alternative lines of ceramic

Once the reflector is constructed, other lines of ceramic free-flooding rings may be inserted if the ceramic rings are not greatly different in size from the initial rings. In this section, we address the performance (both source level and beamwidth) of two alternative lines of ceramic. They are physically one-half and twice the size of the rings described above and, accordingly, have primary frequencies of 15 and 60 kHz, respectively. The length of the line is, however, held constant.

To calculate the performance, we must (1) get estimates of $\overline{\alpha}$, (2) recalculate the ka and hence the DI, as well as the Rayleigh distance r_0, and (3) recalculate the primary source level noting the changes in (a) element size and (b) number of elements. With all this in hand, we then turn to the design curves of Mellen and Moffett as we did above

Table 1: *Predicted difference-frequency source levels and beamwidth for line-in-cone parametric array with 30 kHz primary frequency.*

f_1/f_d	$SL_d - SL_1$ @$SL_1^* = 276$	ΔDI @$SL_1^* = 276$	f_d (Hz)	SL_d dB//1μPa	3 dB Beamwidth
3	−21.0	+1.0	10000	219.0	2.9
5	−27.5	0.0	6000	212.5	3.2
7	−31.5		4300	208.5	
10	−36.5	−1.5	3000	203.5	3.8
15	−41.5		2000	198.5	
20	−45.5	−3.0	1500	194.5	4.6
30	−51.5		1000	188.5	
50	−59.0	−5.5	600	181.0	6.1
70	−64.5		430	175.5	
100	−70.0	−8.5	300	170.0	8.6
200	−81.5	−11.0	150	158.5	11.5
500	−97.0	−15.0	75	143.0	18.2

For the twice-size (half the frequency) ceramic ring, the value of $\overline{\alpha}$ is 1.67×10^{-3} dB/m. The *ka* of the projector is 34.56, the *DI* is 29.2 dB (30.8 − 1.6 dB), and the Rayleigh distance is 9.5 m. Thus the value of $\overline{\alpha} r_0$ is 0.0158, which is close to the $\overline{\alpha} r_0 = 0.02$ set of design curves. See Ref. [15]. The primary source level is the next issue. Application of the transducer scaling law indicates that the acoustic power increases as the square of the dimensional increase. Thus for rings with twice the size, we would have four times the power out. There are, however, now half as many rings because the line must be the same length as before. The power is, accordingly, only doubled. Accounting for the 1 dB loss at the reflector, we end up with a primary source level of 237.0 dB. Use of this source level on the $\overline{\alpha} r_0 = 0.02$ set of design curves yields the values listed in Table 2.

For the half-size (twice the frequency) ceramic ring line, the value of $\overline{\alpha}$ is 16.8×10^{-3} dB/m. The *ka* of the projector is 138.2, the *DI* is 41.2 dB (42.8 − 1.6 dB), and the Rayleigh distance is 38.0 m. Using the scaling law outlined above and noting that there are now twice the number of rings yields that the power is half that of the first line. Accounting for the 1 dB loss at the reflector as before, we end up with a primary source level of 243.0 dB. Use of this source level on the $\overline{\alpha} r_0 = 0.5$ set of design curves yields the values listed in Table 3.

The values listed in Tables 2 and 3 should be compared and contrasted with those in Table 1. To aid in the comparison, the values of source level and 3 dB beamwidths are plotted in Figs. 7 and 8. Note that while the source level is almost linear with the logarithm of frequency, the beamwidths are not.

Table 2: *Predicted difference-frequency source levels and beamwidth for line-in-cone parametric array with 15 kHz primary frequency.*

f_1/f_d	$SL_d - SL_1$ @$SL_1^* = 276$	ΔDI @$SL_1^* = 276$	f_d (Hz)	SL_d dB//1μPa	3 dB Beamwidth
3	−24.5	+2.5	5000	212.5	4.8
5	−30.0	+2.0	3000	206.9	5.1
7	−34.0		2143	202.9	
10	−38.0	+1.5	1500	198.9	5.4
15	−42.5		1000	194.4	
20	−46.0	+1.0	750	190.9	5.7
30	−51.0		500	185.9	
50	−57.5	0.0	300	179.4	6.4
70	−62.0		214	174.9	
100	−66.5	−1.5	150	170.4	7.6
200	−76.0	−3.5	75	160.9	9.6
500	−90.0	−6.5	30	146.9	13.2

Table 3: *Predicted difference-frequency source levels and beamwidth for line-in-cone parametric array with 60 kHz primary frequency.*

f_1/f_d	$SL_d - SL_1$ @$SL_1^* = 276$	ΔDI @$SL_1^* = 276$	f_d (Hz)	SL_d dB//1μPa	3 dB Beamwidth
3	−21.0	−3.0	20000	222.0	2.3
5	−28.5	−5.0	12000	214.5	2.9
7	−34.0		8600	209.0	
10	−39.5	−7.5	6000	203.5	3.8
15	−46.0		4000	197.0	
20	−51.0	−10.0	3000	192.0	5.1
30	−57.5		2000	185.5	
50	−66.5	−14.0	1200	176.5	8.1
70	−72.0		860	171.0	
100	−78.0	−17.0	600	165.0	11.4
200	−90.0	−20.0	300	153.0	16.2
500	−106.0	−24.0	120	137.0	25.8

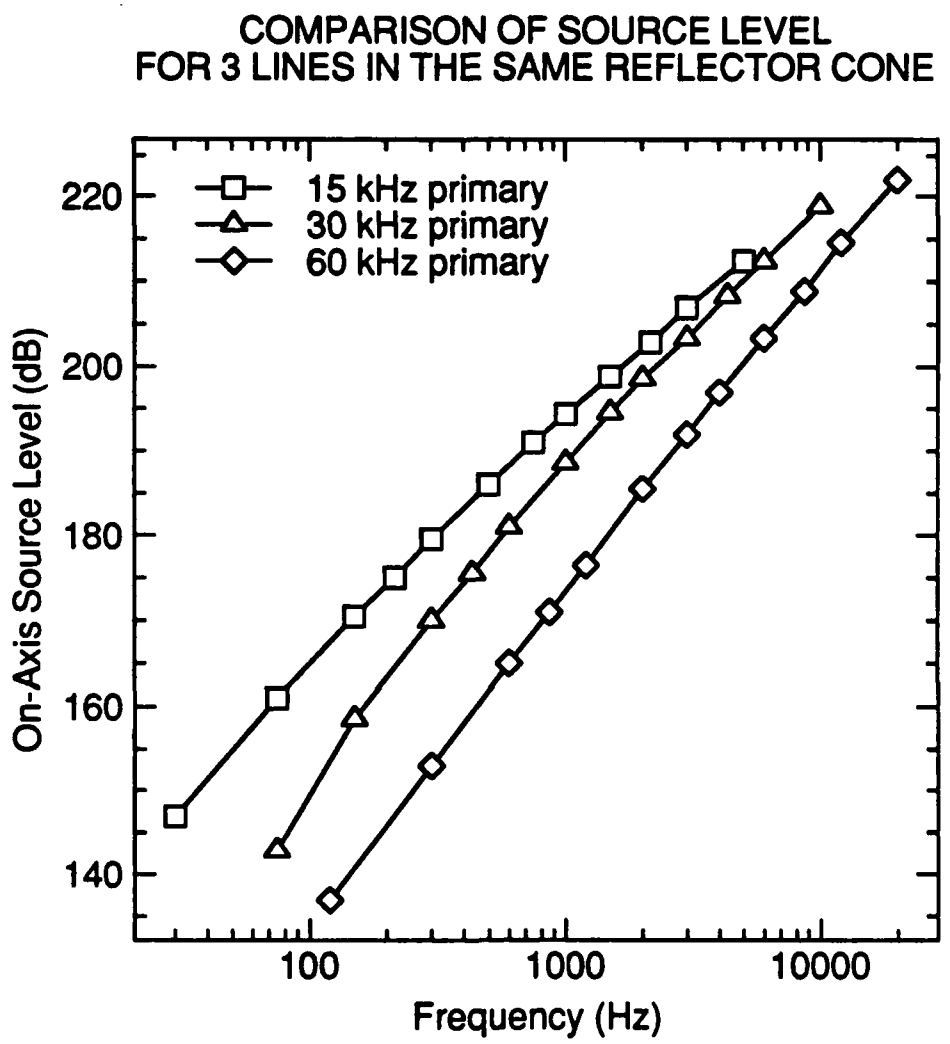

Figure 7: *Plot of source levels versus frequency for the three different lines of ceramic rings in the same reflector cone.*

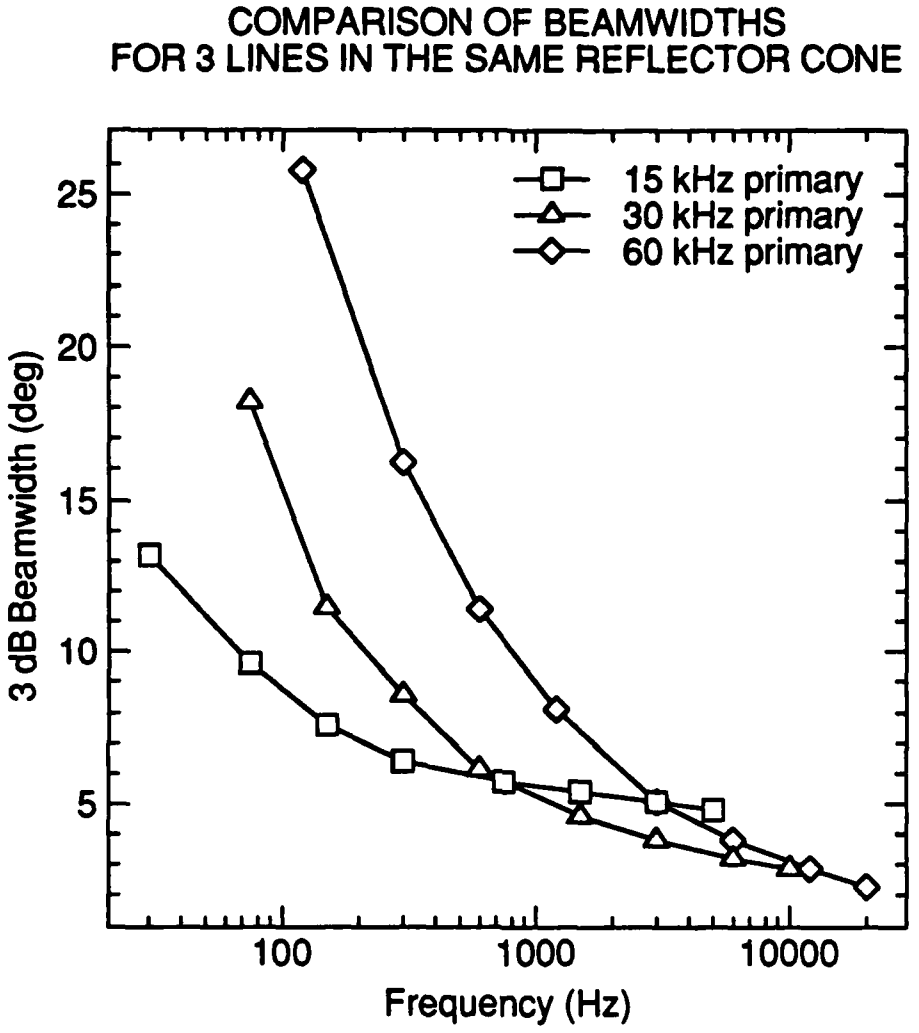

Figure 8: *Plot of 3 dB beamwidth versus frequency for the three different lines of ceramic rings in the same reflector cone.*

6 Summary

In this Technical Memorandum, the fundamentals of the physics that govern the operation of parametric arrays were discussed in a non-mathematical way. The governing relations for a piston source as derived using linear acoustic theory were also discussed. These relations were contrasted with those that govern the source level and beamwidth of the parametric array which is linear absorption limited in the collimated zone near the source. A simple design for a low cost parametric array was presented, and its advantages and disadvantages were discussed.

References

1. D. T. Blackstock,"History of Nonlinear Acoustics and a Survey of Burgers' and Related Equations," in *Nonlinear Acoustics*, edited by T. G. Muir, Proceedings of the Conference on Nonlinear Acoustics, November 1969, Applied Research Laboratories: The University of Texas at Austin, pp. 3–27.

2. L. Euler, *1759 Mem. Acad. Sci. Berlin* **15**, pp. 185–209 (1766).

3. J. Lagrange, "New researches on the nature and propagation of sound," *Misc. Taur.* **2**, pp. 11–172 (1760–61).

4. M. F. Hamilton, "Fundamentals and Applications of Nonlinear Acoustics," in *Nonlinear Wave Propagation in Mechanics*, edited by T. W. Wright, Am. Soc. Mech. Engin. AMD–Vol. 77, Book No. H00346 (1986).

5. P. J. Westervelt, "Parametric acoustic array," *J. Acoust. Soc. Am.* **35**, 535–537 (1963). Reprinted as paper 27 in *Nonlinear Acoustics in Fluids*, edited by R. T. Beyer, Benchmark Papers in Acoustics Series, Van Nostrand Reinhold Co. Inc., New York (1984).

6. H. O. Berktay, "Possible exploitation of non-linear acoustics in underwater transmitting applications," *J. Sound Vib.* **2**, 435–461 (1965). Reprinted, in part, as paper 28 in *Nonlinear Acoustics in Fluids*, edited by R. T. Beyer, Benchmark Papers in Acoustics Series, Van Nostrand Reinhold Co. Inc., New York (1984).

7. H. O. Berktay, "Parametric amplification by the use of acoustic non-linearities and some possible applications," *J. Sound Vib.* **2**, 462–470 (1965). Reprinted as paper 29 in *Nonlinear Acoustics in Fluids*, edited by R. T. Beyer, Benchmark Papers in Acoustics Series, Van Nostrand Reinhold Co. Inc., New York (1984).

8. D. T. Blackstock, "Nonlinear Acoustics (Theoretical)," in *American Institute of Physics Handbook*, 3rd ed., edited by D. E. Gray, pp. 3–183 to 3–205, McGraw-Hill Book Co., Inc., New York (1972).

9. L. E. Kinsler, A. R. Frey, A. B. Coppens, and J. V. Sanders, *Fundamentals of Acoustics*, 3rd ed., John Wiley and Sons, Inc., New York (1982).

10. J. Naze Tjøtta and S. Tjøtta, "Interaction of sound waves. Part III: Two real beams," *J. Acoust. Soc. Am.* **83**, 487–495 (1988).

11. M. B. Moffett and R. H. Mellen, "On parametric source aperture factors," *J. Acoust. Soc. Am.* **60**, 581–583 (1976).

12. M. B. Moffett and R. H. Mellen, "Model for parametric acoustic sources," *J. Acoust. Soc. Am.* **61**, 325–337 (1977).

13. M. B. Moffett, R. H. Mellen, and W. L. Konrad, "Parametric acoustic sources of rectangular aperture," *J. Acoust. Soc. Am.* **63**, 1326–1331 (1978).

14. W. L. Konrad, "Design and performance of parametric sonar systems," NUSC Technical Report 5227, Naval Underwater Systems Center, New London, CT (1975). Reprinted in *Scientific and Engineering Studies: Nonlinear Acoustics 1954 to 1983*, Naval Underwater Systems Center, New London, CT (1984).

15. M. B. Moffett and R. H. Mellen, "Parametric sonar characteristics for circular and square piston projectors," Naval Underwater Systems Center (1976). Reprinted in *Scientific and Engineering Studies: Nonlinear Acoustics 1954 to 1983*, Naval Underwater Systems Center, New London, CT (1984).

16. F. H. Fisher and V. P. Simmons, "Sound absorption in sea water," *J. Acoust. Soc. Am.* **62**, 558–564 (1977).

17. R. P. Chapman, O. Z. Bluy, A. E. Robison, and R. H. Adlington, "Acoustic backscattering measurements in the AFAR area," Defence Research Establishment Atlantic Rept. 71/4 (1971).

18. R. P. Chapman, O. Z. Bluy, R. H. Adlington, and A. E. Robison, "Deep scattering layer spectra in the Atlantic and Pacific oceans and adjacent seas,"*J. Acoust. Soc. Am.* **56**, 1722–1734 (1974).

19. R. H. Mellen and D. G. Browning, "Reflection from a pressure-release surface," *J. Acoust. Soc. Am.* **44**, 646–647 (1968).

20. G. W. McMahon, "Performance of open ferroelectric ceramic cylinders in underwater transducers," *J. Acoust. Soc. Am.* **36**, 528–533 (1964).

21. P. M. Morse, *Vibration and Sound*, 2rd (paperback) ed., American Institute of Physics (1981).

UNCLASSIFIED

SECURITY CLASSIFICATION OF FORM
(highest classification of Title, Abstract, Keywords)

DOCUMENT CONTROL DATA

(Security classification of title, body of abstract and indexing annotation must be entered when the overall document is classified)

1. ORIGINATOR (the name and address of the organization preparing the document. Organizations for whom the document was prepared, e.g. Establishment sponsoring a contractor's report, or tasking agency, are entered in section 8.)

Defence Research Establishment Atlantic
P.O. Box 1012, Dartmouth, N.S. B2Y 3Z7

2. SECURITY CLASSIFICATION (overall security classification of the document, including special warning terms if applicable)

Unclassified

3 TITLE (the complete document title as indicated on the title page. Its classification should be indicated by the appropriate abbreviation (S,C,R or U) in parentheses after the title.)

A Design Proposal for an Inexpensive Parametric Array

4. AUTHORS (Last name, first name, middle initial. If military, show rank, e.g. Doe, Maj. John E.)

Cotaras, F.D.

5. DATE OF PUBLICATION (month and year of publication of document)	6a. NO. OF PAGES (total containing information. Include Annexes, Appendices, etc.)	6b. NO. OF REFS (total cited in document)
January 1991	32	21

6. DESCRIPTIVE NOTES (the category of the document, e.g. technical report, technical note or memorandum. If appropriate, enter the type of report, e.g. interim, progress, summary, annual or final. Give the inclusive dates when a specific reporting period is covered.)

Technical Memorandum

8. SPONSORING ACTIVITY (the name of the department project office or laboratory sponsoring the research and development. Include the address.)

9a. PROJECT OR GRANT NO. (if appropriate, the applicable research and development project or grant number under which the document was written. Please specify whether project or grant)	9b. CONTRACT NO. (if appropriate, the applicable number under which the document was written)
1AT-49	

10a. ORIGINATOR 'S DOCUMENT NUMBER (the official document number by which the document is identified by the originating activity. This number must be unique to this document.)	10b. OTHER DOCUMENT NOS. (any other numbers which may be assigned this document either by the originator or by the sponsor)
DREA Technical Memorandum 91/203	

11. DOCUMENT AVAILABILITY (any limitations on further dissemination of the document, other than those imposed by security classification)

(X) Unlimited distribution
( ) Distribution limited to defence departments and defence contractors; further distribution only as approved
( ) Distribution limited to defence departments and Canadian defence contractors; further distribution only as approved
( ) Distribution limited to government departments and agencies; further distribution only as approved
( ) Distribution limited to defence departments; further distribution only as approved
( ) Other (please specify):

12.. DOCUMENT ANNOUNCEMENT (any limitations to the bibliographic announcement of this document. This will normally correspond to the Document Availability (11). However, where futher distribution (beyond the audience specified in 11) is possible, a wider announcement audience may be selected.)

UNCLASSIFIED

SECURITY CLASSIFICATION OF FORM

DCD03 2/06/87

13. ABSTRACT (a brief and factual summary of the document. It may also appear elsewhere in the body of the document itself. It is highly desirable that the abstract of classified documents be unclassified. Each paragraph of the abstract shall begin with an indication of the security classification of the information in the paragraph (unless the document itself is unclassified) represented as (S), (C), (R), or (U). It is not necessary to include here abstracts in both official languages unless the text is bilingual).

In this Technical Memorandum, the fundamentals of the physics that govern the operation of parametric arrays are discussed in a non-mathematical way. The governing relations for a piston source as derived using linear theory are also discussed. These relations are contrasted with those that govern the source level and beamwidth of the parametric array which is linear absorption limited in the collimated zone near the source. A simple design for a low cost parametric array is presented, and its advantages and disadvantages are discussed.

14. KEYWORDS, DESCRIPTORS or IDENTIFIERS (technically meaningful terms or short phrases that characterize a document and could be helpful in cataloguing the document. They should be selected so that no security classification is required. Identifiers, such as equipment model designation, trade name, military project code name, geographic location may also be included. If possible keywords should be selected from a published thesaurus, e.g. Thesaurus of Engineering and Scientific Terms (TEST) and that thesaurus-identified. If it not possible to select indexing terms which are Unclassified, the classification of each should be indicated as with the title)

Nonlinear Acoustics
Underwater Acoustics
Parametric Array
Nonlinear Sonar